

# Molecular-Dynamics Simulation of Hard-Sphere Fluids with 15% Size Polydispersity<sup>1</sup>

Eri KOHIRA<sup>2</sup>, Yayoi TERADA<sup>3</sup> and Michio TOKUYAMA<sup>4</sup>

## Summary

We perform the extensive molecular-dynamics simulations of hard-sphere fluids. The stable supercooled liquid state is obtained at high volume fraction on the 15% polydisperse hard-sphere fluids, as the volume fraction is increased. It is shown that the static properties and the dynamic properties, such as, the pressure, the long-time self-diffusion coefficient, the non-Gaussian parameter and the self intermediate scattering function in a supercooled liquid state and a liquid state.

## 1. Introduction

On the monodisperse hard-sphere fluids, there exist a stable liquid state, a metastable coexistence state, and a stable crystal state [1, 2, 3, 4]. On the other hand, there exist a stable equilibrium liquid state, a supercooled liquid state, a crystal state, and a metastable supercooled liquid state on hard-sphere fluids with 6% size polydispersity, as the volume fraction is increased. Recently we have shown that the crystallization occurs at those metastable supercooled liquid state for finite long waiting time [5, 6].

In this paper, we perform the molecular-dynamics simulations of hard-sphere fluids with 15% polydispersity that is expected to avoid the crystallization. The stable supercooled liquid state has been obtained within our long-time simulation time. we discuss those supercooled liquid state and liquid state by analyzing the non-Gaussian parameter and the self intermediate scattering function.

## 2. Model

We consider systems which consist of  $N = 10976$  polydisperse and monodisperse hard spheres dispersed in a cubic cell with volume  $V$  at temperature  $T$ . Let

$\mathbf{x}_i$ ,  $\mathbf{v}_i$ , and  $m_i (= 4\pi a_i^3 \rho / 3)$  represent a position vector, a velocity vector, and a mass of  $i$ th sphere respectively, where  $a_i$  denotes the radius of  $i$ th sphere and  $\rho$  a mass density. The distribution of the sphere's radius obeys the Gaussian distribution with standard deviation  $s = 0.15$  for the 15% polydisperse system and  $s = 0$  for the monodisperse system. Here the radius  $a_i$  is set as  $(1 - 3s)a < a_i < (1 + 3s)a$ , where  $a$  denotes the mean radius defined by  $a = \frac{1}{N} \sum_{i=1}^N a_i$ .

The control parameter is given by the volume fraction  $\phi$  defined as

$$\phi = \frac{4\pi}{3} \frac{1}{V} \sum_{i=1}^N a_i^3. \quad (1)$$

The hard spheres in the system continue linear and constant motion except to collide with other spheres. The energy and the momentum in the system are kept constant, because we assume that spheres make perfectly elastic collisions.

We try to prepare two kinds of initial configurations of spheres, the face-centered cubic (FCC) configuration (Fig. 1(a)) and a random configuration (Fig. 1(b)) [7]. However the spheres can not be arranged at the FCC lattice points in higher volume fractions for the 15% polydisperse system. It indicates that there does not exist the FCC crystal state in the system. Therefore we set the initial configurations of the 15% polydisperse system as only the random configuration. Here the periodic boundary condition is employed in order to simulate a bulk system.

---

1. Manuscript received on April 26, 2007.  
2. Student, Graduate School of Engineering, Tohoku University.  
3. Research Associate, Institute Fluid Science, Tohoku University.  
4. Professor, Institute Fluid Science, Tohoku University.

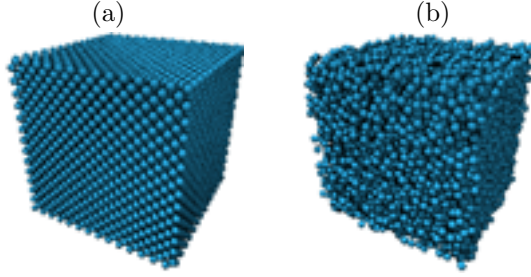


Fig.1 Initial configuration of hard spheres. (a)Face-centered cubic configuration and (b) random configuration.

The unit of the velocity is given by

$$v_0 = \sqrt{\frac{3k_B T}{m}}, \quad (2)$$

where  $k_B$  denotes the Boltzmann constant and  $m$  the mean mass of spheres. The unit of length is the mean radius of spheres  $a$ . The unit of time is given by

$$t_0 = \frac{a}{v_0}. \quad (3)$$

In the following, all physical quantities are divided by those characteristic values in our simulation.

### 3. Physical quantities

We calculated the pressure  $P$ , the mean-square displacement  $M_2(t)$ , the self intermediate scattering function  $F_s(t)$ , and the non-Gaussian parameter  $\alpha_2(t)$  in order to understand the behaviour of hard sphere system.

The pressure is calculated by

$$\frac{PV}{Nk_B T} = 1 - \frac{2}{3Nk_B T \Delta t} \sum_{\text{collision}}^{C_n} \left\langle \frac{m_i m_j}{m_i + m_j} \mathbf{v}_{ij} \cdot \mathbf{x}_{ij} \right\rangle. \quad (4)$$

Here  $C_n$  denotes the number of collisions in time interval  $\Delta t$ ,  $\mathbf{v}_{ij}(= \mathbf{v}_i - \mathbf{v}_j)$  relative velocity and  $\mathbf{x}_{ij}(= \mathbf{x}_i - \mathbf{x}_j)$  relative position where subscripts  $ij$  denote that  $i$ th sphere collides with  $j$ th sphere in  $\Delta t$ . The brackets denotes the ensemble average. The mean-square displacement is calculated by

$$M_2(t) = \frac{1}{N} \sum_{i=1}^N \langle |\mathbf{x}_i(t) - \mathbf{x}_i(0)|^2 \rangle. \quad (5)$$

The long-time self-diffusion coefficient is defined by

$$D_s^L = \lim_{t \rightarrow \infty} \frac{M_2(t)}{6t}. \quad (6)$$

It indicates how easy for spheres to diffuse. The self intermediate scattering function is defined by

$$F_s(\mathbf{k}, t) = \frac{1}{N} \sum_{i=1}^N \exp(-i\mathbf{k} \cdot \{\mathbf{x}_i(t) - \mathbf{x}_i(0)\}), \quad (7)$$

where  $\mathbf{k}$  is the wave vector. In the case of the isotropic system, it is calculated by

$$F_s(k, t) = \frac{1}{N} \sum_{i=1}^N \frac{\sin(k|\mathbf{x}_i(t) - \mathbf{x}_i(0)|)}{k|\mathbf{x}_i(t) - \mathbf{x}_i(0)|}, \quad (8)$$

where  $k(= |\mathbf{k}|)$  denotes the wave number. The non-Gaussian parameter is calculated by

$$\alpha_2(t) = \frac{3}{5} \frac{M_4(t)}{M_2(t)^2} - 1, \quad (9)$$

where  $M_4(t)$  is the mean-fourth displacement.

### 4. Simulation results

Figure 2 shows the results of the mean-square displacement for the 15% polydisperse system. At the short time region,  $M_2(t)$  is proportional to  $t^2$ . It means that the spheres show ballistic motion. On the other hand,  $M_2(t)$  is proportional to  $t$  due to the diffusive motion at the long time region. At the intermediate time region, the cage effect can be seen at high volume fraction. Here the sphere is hard to move because it is surrounded by other strong interacting spheres like the cage, which is called the cage effect. As the volume

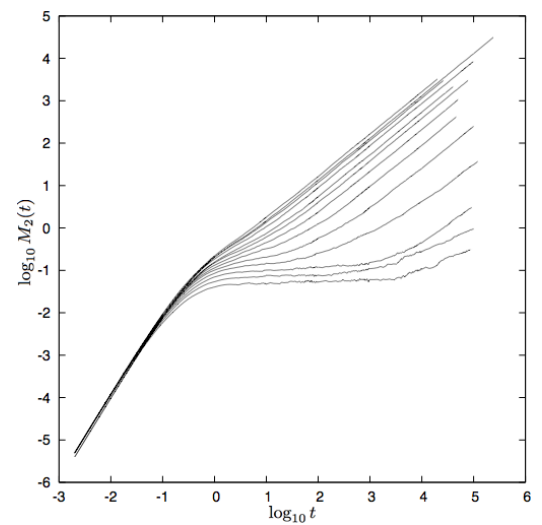


Fig.2 A log-log plot of the mean-square displacement versus time.  $\phi = 0.500, 0.510, 0.520, 0.530, 0.540, 0.550, 0.560, 0.570, 0.580, 0.590, 0.600, 0.610,$  and  $0.620$  (from left to right).

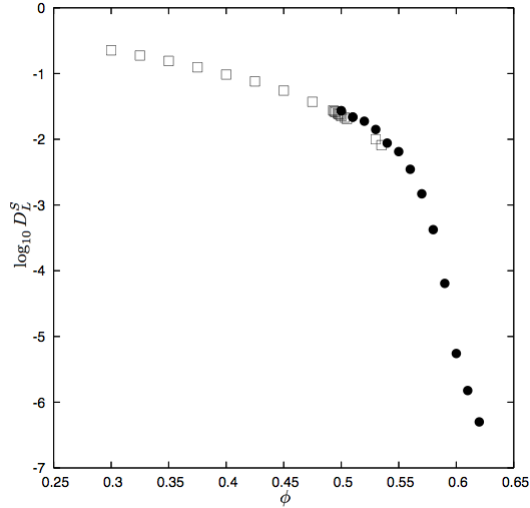


Fig.3 A semi-log plot of the long-time self-diffusion coefficient versus the volume fraction. Filled circles indicates the simulation results of the 15% polydisperse system and open square monodisperse system.

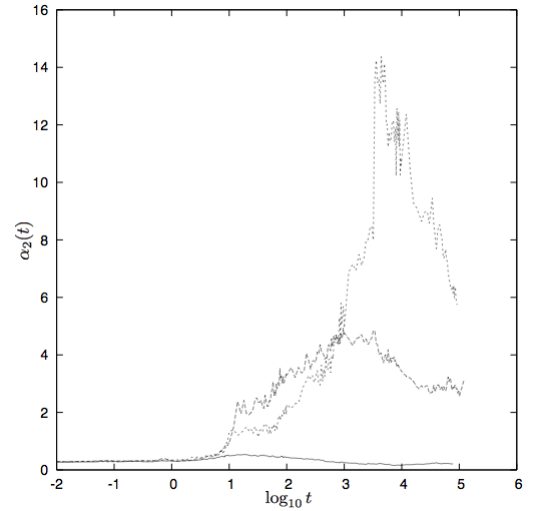


Fig.5 A semi-log plot of the non-Gaussian parameter versus time. The solid line indicates the simulation results at  $\phi = 0.550$ , the dashed line  $\phi = 0.590$ , and the dotted line  $\phi = 0.600$ .

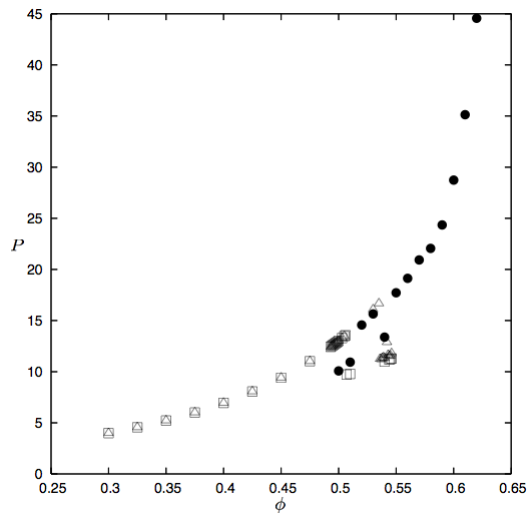


Fig.4 A plot of the pressure versus the volume fraction. Filled circles indicate the simulation results of the 15% polydisperse system, open squares those of the monodisperse system started from FCC configuration, and open triangles those of the monodisperse system started from random configuration.

fraction is increased, the cage effect becomes strong and it takes longer time for the spheres to go through the cage. Therefore the length of the intermediate time region is extended at the high volume fraction. Nevertheless, the crystallization does not occur and there exists the diffusive motion at long time region at the high volume fraction on the 15% polydisperse system.

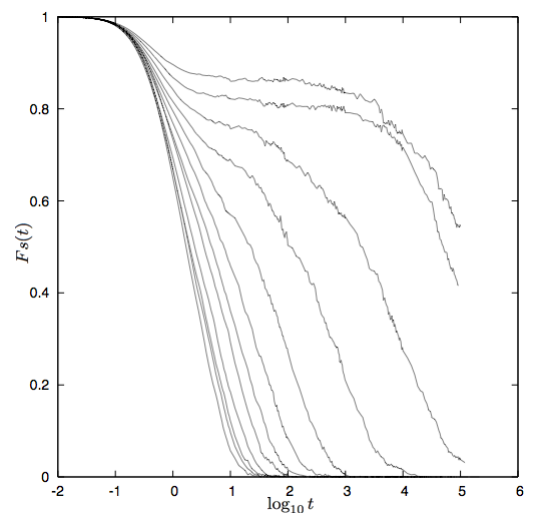


Fig.6 A semi-log plot of the self intermediate scattering function versus time.  $\phi = 0.500, 0.510, 0.520, 0.530, 0.540, 0.550, 0.560, 0.570, 0.580, 0.590, 0.600, 0.610, \text{ and } 0.620$  (from left to right). The wave number is 3.53.

The simulation results of the long-time self-diffusion coefficient  $D_s^L$  are shown in Fig.3. It decreases as the volume fraction is increased. On the monodisperse system,  $D_s^L$  can be obtained till  $\phi = 0.535$ , because the crystallization occurs for  $\phi > 0.535$ . On the other hand, we can obtain  $D_s^L$  for  $\phi > 0.535$  on the 15% polydisperse system because the crystallization does not occur. In addition to that,  $D_s^L$  on the 15% polydisperse system is larger than that on the

monodisperse system for  $\phi < 0.535$ . The spheres are therefore easier to diffuse on the 15% polydisperse system than the monodisperse system. We note that  $D_s^L$  on both systems decreases rapidly around  $\phi = 0.550$ .

Figure 4 shows the simulation results of the pressure. On the polydisperse system, several unstable jumps of the pressure can be seen near the transition points of the monodisperse system. Despite those jumps,  $D_s^L$  shows smooth decrease with increasing volume fraction  $\phi$  in Fig. 3. This is because it is difficult to reach an equilibrium state for the 15% polydisperse system at high volume fraction within our simulation time. We note that the freezing point  $\phi_f = 0.506$  and the melting point  $\phi_m = 0.535$  on the monodisperse case in the present simulation.

The simulation results of the non-Gaussian parameter for the 15% polydisperse system  $\alpha_2(t)$  are shown in Fig. 5. As the volume fraction is increased, the position of peaks is shifted to the long time and the value of peak height becomes large. This increase of the peak height indicates that the spatial structure of the system is heterogeneous at high volume fractions. Here we also could not find the jump of the peak height with increasing the volume fractions. The change of the  $\alpha_2(t)$  with the increase of the volume fraction is continuous.

Finally the simulation results of the self intermediate scattering function are shown in Fig. 6. Here the wave number  $k$  is 3.53. It is determined by the first peak position of the static structure factor. At the low volume fraction, the self intermediate scattering functions obey the exponential decay. At the higher volume fraction, the shoulders can be seen because the correlation of density fluctuation is kept by the cage effect in the intermediate time region. Those shoulders of the self intermediate scattering function are known as the characteristics of a supercooled liquid state.

## 5. Conclusions

The supercooled liquid state has been obtained by performing the molecular-dynamics simulation of the 15% polydisperse hard-sphere fluids with 10976 spheres. We can see the supercooled liquid state clearly by analyzing the self intermediate scattering function and non-Gaussian parameter. In addition to that, the jump of the physical quantities except for the pressure has not seen with increasing the volume fraction on the 15% polydisperse system due to avoid-

ing the crystallization. The detailed crossover phenomena from a liquid phase to a supercooled liquid will be discussed elsewhere. It is noted that we performed the present simulations from only one initial random configuration at each volume fraction. Therefore the unstable jump of the pressure is possibly due to observing the pressure on a metastable state from the specific initial configuration within our simulation time. In the future work, the simulation will be done for the several initial configuration and the ensemble average for the simulation results will be taken.

## Acknowledgements

This work was partially supported by Grants-in-aid for Science Research with No.(C)18540363 from Ministry of Education, Culture, Sports, Science and Technology of Japan. The calculations were performed using the SGI Altix3700Bx2 and NEC SX-8/64M8 in Advanced Fluid Information Research Center, the Institute of Fluid Science, Tohoku University.

## References

- [1] B. J. Alder and T. E. Wainwright: Phase Transition for a Hard Sphere System, *J. Chem. Phys.*, Vol.27 (1957), pp.1208-1209.
- [2] B. J. Alder and T. E. Wainwright: Studies in Molecular Dynamics. I. General Method, *J. Chem. Phys.*, Vol.31 (1959), pp.459-466.
- [3] M. D. Rintoul and S. Torquato: Metastability and Crystallization in Hard-Sphere Systems, *Phys. Rev. Lett.*, Vol.77 (1996), pp.4198-4201.
- [4] M. D. Rintoul and S. Torquato: Computer Simulation of Dense Hard-Sphere Systems, *J. Chem. Phys.*, Vol.105 (1996), pp.9258-9265.
- [5] M. Tokuyama and Y. Terada: Slow Dynamics and Re-entrant Melting in a Polydisperse Hard-sphere Fluid, *J. Phys. Chem. B*, Vol.109 (2005), pp.21357-21363.
- [6] M. Tokuyama and Y. Terada: How Different is a Hard-sphere Fluid from a Suspension of Hard-sphere Colloids near the Glass Transition?, *Physica A*, Vol.375 (2007), pp.18-36.
- [7] W. S. Jodrey and E. M. Tory: Computer Simulation of Close Random Packing of Equal Spheres *Phys. Rev. E*, Vol.32 (1996), pp.2347-2351.